The Clouds of Venus: I. An Approximate Technique for Treating the Effects of Coagulation, Sedimentation and Turbulent Mixing on an Aerosol [1]

WILLIAM B. ROSSOW

Geophysical Fluid Dynamics Program, Princeton University, Princeton, N.J. 08540

PETER J. GIERASCH

Laboratory for Planetary Studies, Cornell University, Ithaca, N.Y. 14853

(Manuscript received 5 March 1976, in revised form 30 August 1976)

ABSTRACT

An approximate technique is presented for calculating the size distribution of an aerosol under Venus conditions using the first three moments of the distribution. The effects of coagulation, sedimentation and turbulent mixing are included. The approximate solution is compared to more accurate numerical solutions. The method is sufficiently accurate and fast to be useful in large-scale dynamic calculations of the Venus atmosphere. Using this method, we place upper limits on the dust number density in the Venus atmosphere from a meteoritic source.

1. Introduction

The Venus clouds are 30–40 km deep (Marov *et al.*, 1973) and control both the shortwave and longwave radiation fluxes. Since radiative heating is the drive for motions, complete dynamical calculations must include the effects of microphysical processes and atmospheric motions of all scales on the distribution of cloud aerosols and particle sizes in order to model the radiation field properly. In this paper we present an approximate technique for calculating the aerosol size distribution under Venus conditions using the first three moments of the distribution. The method is reasonably accurate and both computationally and conceptually simple.

The Venus clouds are composed of a strong solution of sulfuric acid (Young, 1975). Since the vapor pressure over a sulfuric acid droplet is more sensitive to changes in the concentration than to changes in droplet size, the droplets are stabilized against vapor exchanges. Thus, except for the initial formation of the droplets, condensation has a negligible effect on the size distribution. The only remaining process which affects the droplet size distribution in the bulk of the cloud far from the formation region is collisions between droplets (Rossow, 1977).

The fundamental equation determining an aerosol size distribution under the influence of collisions is

$$\frac{\partial n(m,t)}{\partial t}=\frac{1}{2}\int_0^m K(m',\,m-m')n(m',t)n(m-m',\,t)dm' - n(m,t)\int_0^\infty K(m,m')n(m',t)dm'+I(m,t), \quad (1)$$

where $n(m,t)$ is the number density of aerosol particles per unit mass interval at time t, $K(m,m')$ is the collision rate coefficient and $I(m,t)$ represents any source or sink of particles in a unit of volume, e.g., $I(m,t)$ can represent condensation.

Collisions between particles occur either because of differences in sedimentation velocities or Brownian motion. Near the 50 mb level on Venus the cloud droplets are very small and nearly uniform in size; the radius is 1.05 ± 0.10 μm (Hansen and Hovenier, 1974). The relative importance of coalescence and coagulation can be evaluated by comparing the time constants (Fuchs, 1964)

$$\frac{1}{\tau_{\text{coag}}}=\frac{1}{N_1}\frac{dN_1}{dt}\approx\frac{4kT}{3\eta}N_2$$

and

$$\frac{1}{\tau_{\text{coal}}}=\frac{1}{N_1}\frac{dN_1}{dt}=\frac{\pi}{2}(a_1+a_2)^2E_{12}(V_1-V_2)N_2,$$

where N_1 and N_2 are the particle concentrations, k is

[1] Work completed while senior author was at Cornell University.

Boltzmann's constant, T the absolute atmospheric temperature, η the atmospheric viscosity, a_1 and a_2 the particle radii, V_1 and V_2 the sedimentation velocities and E_{12} the collision efficiency. For this very narrow size distribution, $a_1 \approx a_2 \approx 1\,\mu$m and $V_1 - V_2 < 0.1 V_1$, giving

$$\frac{\tau_{\text{coag}}}{\tau_{\text{coal}}} < \frac{2}{30} \rho_p \frac{g a_1^4}{kT} E_{12} \sim E_{12},$$

where ρ_p is the droplet mass density. Since $E_{12} \ll 1$ for these small droplets (Klett and Davis, 1973), coalescence is not likely to be an important process in the Venus clouds or for smaller sized aerosols. Therefore, in what follows, we assume that coagulation is the only microphysical process influencing the aerosol size distribution on Venus. The cloud droplets are formed by condensation, but condensation is unimportant in the bulk of the cloud.

Several approximate analytic solutions to Eq. (1) with $I(m,t)=0$ have been found for simple forms of $K(m.m')$ (Drake and Wright, 1972; Friedlander and Wang, 1966; Scott, 1968). Friedlander (1960a,b, 1961) considers steady-state solutions for Brownian coagulation with $I(m,t)$ representing sedimentation. The steady-state solution balances the transfer of mass into a particular size range against the loss of mass by sedimentation. For the smaller particles, coagulation predominates and dimensional analysis gives $n(m) \propto m^{-5/6}$, while for the larger particles, sedimentation predominates and $n(m) \propto m^{-19/12}$ (Friedlander, 1960b). Klett (1975) considers the whole class of steady-state solutions for

$$K(x,y) = K_0 x^\beta y^\beta \quad (0 \leqslant \beta \leqslant 1),$$
$$I(x,t) = I_0[(p+1)^{p+1} x^p e^{-(p+1)x}][m_0 \Gamma(p+1)]^{-1},$$

where p is a positive integer, x and y are dimensionless masses, I_0 is the source strength at mean mass m_0 and Γ is the gamma function.

Only numerical solutions seem possible for the more general forms of Eq. (1), however. These numerical solutions usually involve breaking the size distribution function into a discrete set of functions representing the number of particles in size categories and solving the resulting set of coupled, nonlinear equations (Berry and Reinhardt, 1974; Hidy, 1965; Mockros *et al.*, 1967; Warshaw, 1967). Since the stability and convergence properties of these solutions usually result in complex time-consuming calculations, these methods of solution cannot be conveniently incorporated into existing dynamic model calculations.

Detailed observations of an aerosol size distribution require actually collecting samples, carefully calibrating the collection efficiences of the collectors, and laboriously examining the particles under a microscope in order to size and count them. The collection of liquid aerosol particles presents even more problems. Other observational methods, including those used to observe aerosols on other planets, depend on the optical properties of the aerosols. By observing reflected, transmitted or emitted light at different wavelengths, phase angles and polarizations, a few properties of an aerosol distribution can usually be deduced, but not the detailed distribution function $n(m,t)$ (see, e.g., Hansen and Hovenier, 1974). Thus from an observational as well as computational standpoint, it might be more convenient, in comparing data to theoretical predictions, to recast Eq. (1) in terms of integrated properties of the size distribution such as the total number and mass concentrations and variance of the size distribution.

The purpose of this paper is to derive a relatively simple, approximate method of solving Eq. (1) for conditions appropriate to the Venus clouds, where $I(m,t)$ includes the effects of turbulent mixing and sedimentation. We present the method in Section 2 in the context of a simple, one-dimensional, vertical structure model of the behavior of meteoritic dust in the atmosphere of Venus. The source of particles is then simply a flux of particles at the top of the model atmosphere without the complications of condensation growth. These particles can serve as condensation nuclei for the clouds of Venus, and we shall refer to these results in our second paper (Rossow, 1977). Unlike the cloud droplets which evaporate at the bottom of the cloud, the dust particles are removed at the planetary surface at a rate which depends on the conditions in the atmospheric boundary layer. This particular case requires a specification of the derivatives of the solution (flux) at the bottom boundary rather than the magnitude of the solution. We concentrate our discussion here on these least accurate results produced by the approximations required for the bottom boundary conditions (Section 3). In Section 4 we discuss the qualitative behavior of the solutions to Eq. (1), and in Section 5 we present the solutions of Eq. (1) using a discrete size distribution technique. In Section 6 we compare the results of Section 5 with our approximate solutions and show that the approximate solutions are reasonable accurate and qualitatively correct. Finally, in Section 7 we summarize our conclusions.

2. Equations

Multiplying Eq. (1) by m^ν and integrating over all masses gives (Klett, 1975)

$$\rho \frac{\partial \chi_\nu}{\partial t} = \tfrac{1}{2}\rho^2 \int_0^\infty dm \int_0^\infty dm' [(m+m')^\nu - m^\nu - m'^\nu] K(m,m') \times q(m,t) q(m',t) + \int_0^\infty m^\nu I(m,t) dm, \quad (2)$$

where ρ is the atmospheric density, $K(m,m')$ the Brownian coagulation coefficient and $q(m,t)$ the

number of aerosol particles per gram of atmosphere per mass interval, i.e.,

$$\rho q(m,t)=n(m,t). \tag{3}$$

The quantity χ_ν is defined by

$$\chi_\nu=\int_0^\infty m^\nu q(m,t)dm. \tag{4}$$

Thus χ_0 is the total number and χ_1 the total mass of aerosol particles per gram of atmosphere. The mean mass and the variance of the size distribution are given by

$$\langle m\rangle=\frac{\chi_1}{\chi_0}, \tag{5}$$

$$\sigma^2\equiv\frac{\langle m^2\rangle-\langle m\rangle^2}{\langle m\rangle^2}=\frac{\chi_2\chi_0}{\chi_1^2}-1. \tag{6}$$

$I(m,t)$ is the rate of change of $n(m,t)$ due to sedimentation and turbulent mixing and can be written as (Haltiner and Martin, 1957)

$$I(m,t)=\frac{\partial}{\partial z}\left[\rho E\frac{\partial q(m,t)}{\partial z}+\rho V_s q(m,t)\right], \tag{7}$$

where the turbulent mixing is parameterized by an eddy diffusivity E and V_s is the sedimentation velocity.

In order to solve Eq. (2) for the first three moments of the steady-state size distribution $[(\partial\chi_\nu/\partial t)=0]$, the following assumptions are made:

1) $K(m,m')\approx K_0=\dfrac{8kT}{3\eta}$, (8)

where k is Boltzmann's constant, T the absolute atmospheric temperature and η the atmospheric viscosity.

2) $V_s(m)=cm^{\frac{2}{3}}+c'm^{\frac{4}{3}}$
$\approx\frac{1}{2}c[\langle m\rangle^{\frac{2}{3}}+\langle m\rangle^{-\frac{1}{3}}m]+c'\langle m\rangle^{\frac{4}{3}}$, (9)

where $c=(2\rho_p g/9\eta)(4\pi\rho_p/3)^{-\frac{2}{3}}$, $c'=c(4\pi\rho_p/3)^{\frac{1}{3}}\beta\lambda$, $\langle m\rangle$ is defined by Eq. (5), ρ_p is the mass density of the aerosol particles (assumed to be 2 gm cm^{-3}) and g is the acceleration due to gravity; λ is the gas mean free path and β the Cunningham factor.

3) $\int m^{8/3}q(m)dm\approx f_1\langle m\rangle^{\frac{2}{3}}\chi_2$, (10)

where f_1 is a constant of order unity.

4) $E/H\gtrsim V_s$ [in the lower atmosphere].

a. $K(m,m')\approx K_0$

This assumption neglects the two size-dependent terms in the classical expression for the coagulation coefficient (Fuchs, 1964) which depend on the ratio of m and m' to the one-third power. This is not a serious error for particle size distributions ranging over only a few orders of magnitude in mass. The accuracy of this assumption is corroborated by the results presented in Sections 5 and 6 as well as by numerical solutions to Eq. (1) performed by Mockros *et al.* (1967). This value of $K(m,m')$ assumes that the sticking efficiency is unity which Fuchs (1964) demonstrates is correct for particles $\gtrsim 10^{-7}$ cm in radius.

This assumption also neglects the change in the coagulation rate with atmospheric density. When the gas mean free path is larger than the particle size, the assumption that the gas drag is that of a fluid no longer holds. While the experimental verification of the value of $K(m,m')$ between the region of validity of the classical expression and the region of validity of the gas kinetic expression (Fuchs, 1964) is uncertain, theoretical results (Fuchs, 1964; Hidy and Brock, 1965) have been derived for this transition region. The numerical values are within a factor of 3 of the constant value assumed here. Since the coagulation rate is small in the upper Venus atmosphere where these effects are important, this assumption produces little effect in the results.

b. $V_s(m)\approx\frac{1}{2}c[\langle m\rangle^{\frac{2}{3}}+\langle m\rangle^{-\frac{1}{3}}m]$

In the Stokes regime, the terminal velocity is proportional to $m^{\frac{2}{3}}$ and therefore introduces in (2) an integral of the form

$$\int_0^\infty m^{\nu+\frac{2}{3}}q(m)dm. \tag{11}$$

In order to write (2) entirely in terms of integer moments of the size distribution, this integral is approximated in terms of the mean mass and integer powers of the mass. For particle mass distributions with only a limited mass range, the first term in the brackets in (9) probably represents an underestimate for (11), while the second term represents an overestimate. Note that this form produces a coupled set of equations in (13) and depends only weakly on the mean mass.

As an example of the accuracy of this approximation, Fig. 1 shows the ratio of

$$\tfrac{1}{2}[\langle m\rangle^{\frac{2}{3}}\chi_\nu+\langle m\rangle^{-\frac{1}{3}}\chi_{\nu+1}] \tag{12}$$

and Eq. (11) for $\nu=0, 1, 2$ for power law fits to the two branches of the size distributions of the form $q=q_0m^{-p}$ with $-5\leqslant p\leqslant 5$. The value $p=0$ corresponds to a constant distribution, while $p\to\infty$ corresponds to a delta function for which the approximation is exact. The peaks in the curves shown occur near the values of p for which the integrals in (11) and (12) are a minimum. The height of the peaks is a function of the integration limits chosen since the minimum

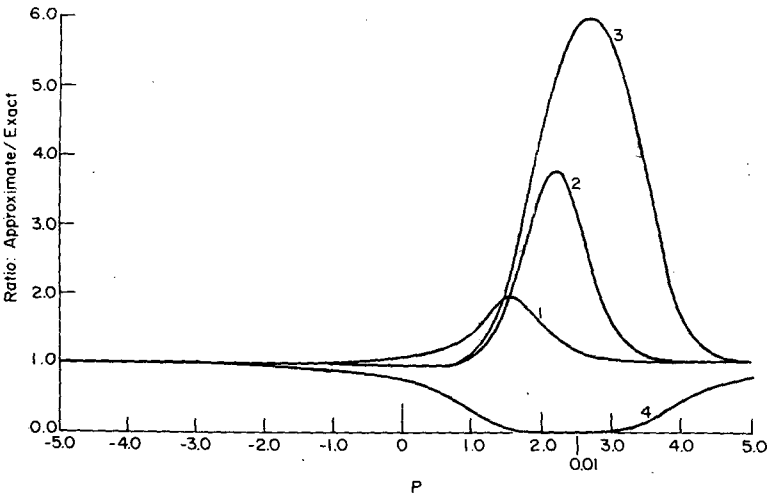

FIG. 1. Ratio of approximate to exact sedimentation terms for power law size distributions. Curves 1, 2 and 3 are ratios for the first three moments and curve 4 is ratio for the closure approximation.

value of the integrals is just $\ln(m_2/m_1)$, where m_2 is the upper integration limit and m_1 the lower limit. For Fig. 1 the ratio of m_2 to m_1 is 10^4. The peaks are smaller if this ratio is smaller.

It can be seen that the approximation in Eq. (9) is generally very good, except for size distribution with $2 \lesssim p \lesssim 4$. Aerosols on Earth are observed to fit power law distributions with $p = 1 \pm \frac{1}{3}$ (Junge, 1963), while general solutions to (1), called similarity solutions and produced by rapid collisions, have $p = 1$ (Liu and Whitby, 1968). Since distributions with $p > 2$ are so sharp that most of the mass is contained near one size, we can reduce the integration limits thereby reducing the peaks in Fig. 1. Thus we expect (9) to be accurate for most naturally occurring unimodal size distributions. Specifically, Hansen and Hovenier's (1974) results for the Venus cloud droplets are consistent with $p \approx 1$. The most inaccurate case that we encounter is a case of strong turbulent mixing throughout the whole depth of the atmosphere with a strong coagulation which produces a broad bimodel distribution.

In the gas kinetic regime, the terminal velocity is such a weak function of particle mass that the simple approximation in the second term of (9) is found to be reasonably accurate.

c. $\int m^{8/3} q(m)\,dm \approx f_1 \langle m \rangle^{\frac{8}{3}} \chi_2$

The approximation in Eq. (9) always introduces the next higher moment in each equation and therefore, this assumption is necessary in order to close the system of equations. The ratio

$$\langle m \rangle^{\frac{8}{3}} \chi_2 \Big/ \int_0^\infty m^{8/3} q(m)\,dm$$

is shown in Fig. 1, curve 4, and indicates that f_1 must be greater than unity. We show in Section 6 that factor of 2 error in f_1 produces less than a factor of 2 error in χ_2 and hardly any error in χ_0 and χ_1.

d. $E/H \gtrsim V_s$

This assumption is required because the particular method we use to solve Eq. (2), described in Section 6, is stable only when this condition is met throughout that part of the atmosphere where the gas mean free path is smaller than the mean particle radius. When this condition is not met, Eq. (2) reduces to a simple first-order equation and a different method of solution must be used. However, for meteoritic dust and cloud droplets on Venus with particle radius $\lesssim 2$ μm, this condition is met by $E \geqslant 10^4$ cm^2 s^{-1}. We consider only cases with $E \geqslant 10^4$ cm^2 s^{-1} in what follows.

With these approximations the set of equations to be solved is

$$\left.\begin{aligned}
&\left\{\frac{\partial}{\partial z}\left[\rho E\frac{\partial}{\partial z} + \tfrac{1}{2}\rho c\langle m\rangle^{\frac{2}{3}} + \rho c'\langle m\rangle^{\frac{1}{3}}\right] - \tfrac{1}{2}\rho^2 K_0 \chi_0\right\}\chi_0 \\
&\qquad + \left\{\frac{\partial}{\partial z}\left[\tfrac{1}{2}\rho c\langle m\rangle^{-\frac{1}{3}}\right]\right\}\chi_1 = 0 \\
&\left\{\frac{\partial}{\partial z}\left[\rho E\frac{\partial}{\partial z} + \tfrac{1}{2}\rho c\langle m\rangle^{\frac{2}{3}} + \rho c'\langle m\rangle^{\frac{1}{3}}\right]\right\}\chi_1 \\
&\qquad + \left\{\frac{\partial}{\partial z}\left[\tfrac{1}{2}\rho c\langle m\rangle^{-\frac{1}{3}}\right]\right\}\chi_2 = 0 \\
&\left\{\frac{\partial}{\partial z}\left[\rho E\frac{\partial}{\partial z} + f_1\rho c\langle m\rangle^{\frac{2}{3}} + \rho c'\langle m\rangle^{\frac{1}{3}}\right]\right\}\chi_2 + \rho^2 K_0 \chi_1^2 = 0
\end{aligned}\right\}. \quad (13)$$

3. Boundary conditions

For the purposes of this paper, the source of aerosol particles is taken to be a given flux at the top of the model atmosphere with the ultimate sink being removal at the planetary surface.

a. Input flux

The input flux size distribution is assumed for discussion to be a delta-function; therefore the boundary conditions at the top of the atmosphere are

$$\left.\begin{aligned}
&\left\{\rho E\frac{\partial}{\partial z}+\tfrac{1}{2}\rho c\langle m\rangle^{\frac{2}{3}}+\rho c'\langle m\rangle^{\frac{1}{3}}\right\}\chi_0 \\
&\qquad\qquad +\tfrac{1}{2}\rho c\langle m\rangle^{-\frac{1}{3}}\chi_1=F_0 \\
&\left\{\rho E\frac{\partial}{\partial z}+\tfrac{1}{2}\rho c\langle m\rangle^{\frac{2}{3}}+\rho c'\langle m\rangle^{\frac{1}{3}}\right\}\chi_1 \\
&\qquad\qquad +\tfrac{1}{2}\rho c\langle m\rangle^{-\frac{1}{3}}\chi_2=F_0 m_0 \\
&\left\{\rho E\frac{\partial}{\partial z}+f_1\rho c\langle m\rangle^{\frac{2}{3}}+\rho c'\langle m\rangle^{\frac{1}{3}}\right\}\chi_2=F_0(m_0)^2
\end{aligned}\right\}, \quad (14)$$

where F_0 is the number flux of particles of mass m_0. A broader distribution can be simulated by adjusting the values of flux terms in the last two equations.

Since the size distribution of interplanetary dust seems to peak near a radius of ~ 0.1 μm (Schneider *et al.*, 1973), we model the dust input as a flux of uniform size grains with radius $a=0.1$ μm. Estimates of the number density of small dust grains near Venus are between a factor of 10 smaller (Rhee, 1968) and a factor of 2 larger (Dohnanyi, 1972) than the number density near Earth. We assume that the dust flux into the Venus atmosphere is comparable to that into Earth's atmosphere. Most previous estimates of this flux, ranging from $\sim 10^7$ tons year^{-1} (Öpik, 1956) to $\sim 10^{-2}$ particles cm^{-2} s^{-1} (Mason, 1971; Junge, 1963), are based on observations of larger particulates ($a \approx 1$ μm) in Earth's atmosphere and hence contain an unknown contribution from the ablation products of larger meteorites. More recent determinations of the meteoritic dust flux onto the moon give values as low as $\sim 10^{-6}$ cm^{-2} s^{-1} (Schneider *et al.*, 1973) and suggest that ablation products dominate the meteoritic dust in Earth's atmosphere. Therefore a flux ~ 1 cm^{-2} s^{-1} of 0.1 μm particles into the atmosphere of Venus is certainly an upper limit.

b. Surface boundary condition

The flux of particles onto the planetary surface is written as a velocity times the concentration, i.e.,

$$F_\nu(\text{surface})=\rho V'\chi_\nu(\text{surface}), \quad (15)$$

where F_ν is the sum of the turbulent flux and the sedimentation flux given by the expressions on the left side of (14). F_ν(surface) is actually evaluated at the top of the atmospheric boundary layer where air motions are not influenced by the presence of the surface. The value of V' is then the transport velocity of particles through this layer to the surface. In general V' can be a function of particle size.

In the steady state, the flux of particles at all points in the boundary layer is the same; therefore, V' is the deposition velocity at the planet's surface independent of the transport through the boundary layer. Davies (1966) considers the detailed physics of aerosol deposition in this layer and his results can be reduced to two cases of interest: turbulent deposition or gravitational sedimentation. For a very rough surface and fully developed turbulence, Davies' results give a deposition rate comparable to the velocity in the turbulent eddies near the surface. For this case, the deposition velocity is of order U_*, the friction velocity. In the case of no wind or very small winds, deposition occurs by gravitational sedimentation and V' is then the terminal velocity of the particles. This general qualitative behavior has been observed experimentally by Gillette *et al.* (1972), Gillette *et al.* (1974) and Gillette and Goodwin (1974).

c. Approximate boundary condition in Stokes case

When V' is size-dependent, we must introduce approximations similar to those discussed in Section 2. In this particular case, V' is the Stokes sedimentation velocity and the approximations (9) and (10) must be used. Thus an assumption about the size distribution at the surface is introduced by choosing a particular value of f_1 in Eq. (10).

However, for steady-state solutions, a procedure was found to make the bottom boundary condition less sensitive to the assumptions about the size distribution. The procedure, for the particular example of a Stokes velocity, is as follows: since coagulation conserves mass, there is no coagulation term in the equation for χ_1 in (13). Thus we may integrate this equation using the top boundary condition (14). Setting V' equal to the Stokes velocity, we obtain

$$\langle m\rangle^{\frac{2}{3}}\chi_1+\langle m\rangle^{-\frac{1}{3}}\chi_2=\frac{2F_0 m_0}{\rho c}. \quad (16)$$

The ratio of the terms on the left is

$$\frac{\chi_2}{\chi_1}\langle m\rangle^{-1}=\sigma^2+1. \quad (17)$$

Since the minimum value of σ^2 is zero, there is a lower bound on χ_2. From Eq. (16) there is an upper bound, and these limits imply

$$\frac{F_0 m_0}{\rho c}\leqslant\langle m\rangle^{-\frac{1}{3}}\chi_2\leqslant\frac{2F_0 m_0}{\rho c}. \quad (18)$$

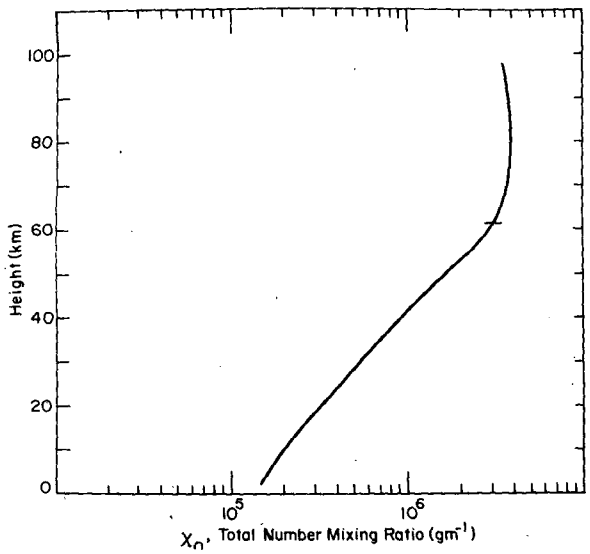

FIG. 2. Total number mixing ratio as a function of altitude with no turbulent mixing.

This information can be used to rewrite (16) as two boundary conditions in terms of the parameter γ:

$$\langle m\rangle^{-\frac{1}{3}}\chi_2=\gamma\frac{F_0m_0}{\rho c}, \tag{19}$$

$$\langle m\rangle^{\frac{1}{3}}\chi_1=(2-\gamma)\frac{F_0m_0}{\rho c}, \tag{20}$$

where γ is given by

$$\gamma=1+\frac{\sigma^2}{\sigma^2+2}. \tag{21}$$

Notice that $1\leqslant\gamma\leqslant 2$. By specifying γ, an assumption about the variance of the size distribution at the surface is introduced, but the results are not very sensitive to the choice of γ, as is illustrated in Section 6.

Unfortunately, this procedure cannot be used in a time-dependent calculation since Eq. (13) for χ_1 cannot be integrated. However, the Stokes boundary condition is almost certainly not the one of interest on Venus, where the Stokes velocity is extremely small at the surface. We have dealt with this case here for completeness.

4. Qualitative behavior of solutions

a. Coagulation neglected

We first consider solutions for which the coagulation terms are negligible compared to the mixing and sedimentation terms; i.e., $\tau_{coag}\gg\tau_s$, τ_E, where the time constants are defined by

$$\left.\begin{aligned}\tau_{coag}&=[\tfrac{1}{2}\rho^2K_0\chi_0^2]^{-1}\\ \tau_s&=H/V_s\\ \tau_E&=H^2/E\end{aligned}\right\}, \tag{22}$$

where H is the scale height of the atmosphere. When coagulation can be neglected, the mean mass $\langle m\rangle$ is constant with altitude.

We now consider the cases where each of the two remaining terms predominate.

(i) $\tau_s\ll\tau_E$

Neglecting the coagulation and turbulent mixing terms and integrating Eq. (13) once using the boundary condition (14) gives

$$\left.\begin{aligned}\chi_0&=2F_0\left[2+\frac{c'}{c}m_0^{-\frac{1}{3}}\right]^{-1}\\ \chi_1&=\left[\frac{2F_0m_0^{\frac{1}{3}}}{\rho c}-\frac{\chi_2}{m_0}\right]\left[1+\frac{c'}{c}m_0^{-\frac{1}{3}}\right]^{-1}\\ \chi_2&=\frac{F_0m_0^{\frac{1}{3}}}{\rho c}\left[f_1+\frac{c'}{c}m_0^{-\frac{1}{3}}\right]^{-1}\end{aligned}\right\}, \tag{23}$$

remembering the definition of $\langle m\rangle$ from Eq. (5). When the gas mean free path is smaller than the particle radius (i.e., $(c'/c)m_0^{-\frac{1}{3}}\ll 1$), all the χ_ν's are proportional to ρ^{-1}. When the gas mean free path is much larger than the particle size, the sedimentation velocity becomes proportional to ρ since $c'\propto\rho$ so that the χ_ν's are constant with altitude. This behavior is illustrated in Fig. 2, where the Cunningham correction to the sedimentation velocity has been included. The level at which the mean free path is equal to the particle size is marked.

(ii) $\tau_E\ll\tau_s$

Integrating (13) once and using the boundary condition (14) gives

$$\rho E\frac{\partial\chi_\nu}{\partial z}=F_0(m_0)^\nu. \tag{24}$$

Assuming for simplicity that E is constant and $\rho=\rho_0\exp(-z/H)$, this equation has a solution

$$\chi_\nu=\chi_\nu(0)+\frac{F_0(m_0)^\nu H}{E}\left(\frac{1}{\rho}-\frac{1}{\rho_0}\right), \tag{25}$$

where $\chi_\nu(0)$, the value of χ_ν at the surface, is given by the bottom boundary condition. There are two cases. If V' in (15) satisfies $V'\gg E/H$, then χ_ν is proportional to $(\rho^{-1}-\rho_0^{-1})$ as shown by curve c in Fig. 3. If $V'\ll E/H$, then $\chi_\nu(0)\gg F_0(m_0)^\nu H/E$, and χ_ν is constant up to some height where the ρ^{-1} behavior begins to dominate. This behavior is illustrated by curves a and b in Fig. 3, where the Cunningham correction to the terminal velocity has been neglected in order to show the transition more clearly. The tick marks indicate that level at which $\chi_0(0)=F_0H/\rho E$.

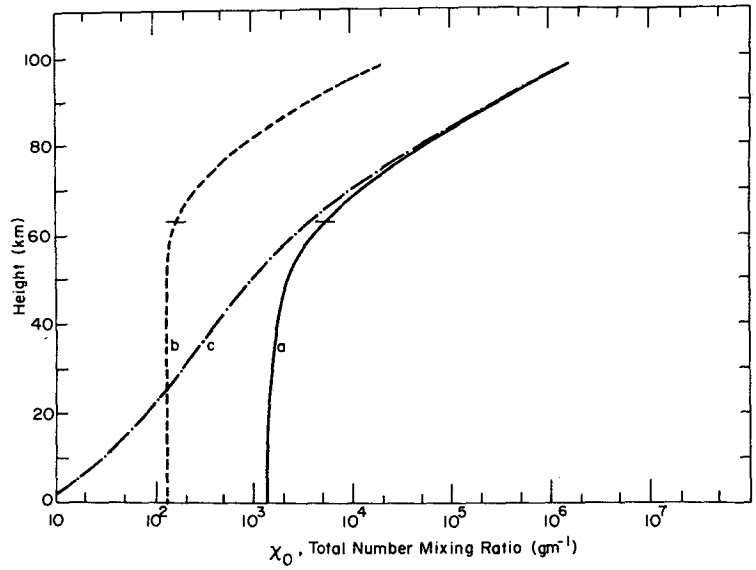

FIG. 3. As in Fig. 2 with $E=10^4$ cm^2 s^{-1}. Curves a and b are for different flux boundary conditions.

b. Source term neglected

We next consider solutions to Eq. (2) for which sedimentation and mixing are neglected. These solutions are not steady-state solutions, but Friedlander and Wang (1966) have shown that, after a long time compared to τ_{coag}, the nondimensional shape function defined by

$$\Psi(\eta)\equiv\frac{n(m,t)\chi_1}{\chi_0^2},\quad \eta\equiv\frac{m\chi_0}{\chi_1},$$

becomes independent of time. Thus, while the mean mass increases in time, the variance of the size distribution is equal to 1 and constant. Coagulation thereby acts to broaden size distributions with $\sigma^2<1$ and to narrow size distributions with $\sigma^2>1$.

c. Full solution

Finally we consider solutions of Eq. (13) which are a balance between the transport rates and the coagulation rates. Since coagulation reduces the particle number density, thereby increasing τ_{coag}, steady-state solutions require $\tau_{coag}\gtrsim\tau_E$ or τ_s. In the case $\tau_s\ll\tau_E$, the balance between coagulation and sedimentation produces a size distribution in which the mass transfer through the size distribution is limited by the removal of larger particles by sedimentation. This is the result found by Friedlander (1960a,b, 1961). In the case $\tau_E\ll\tau_s$, the balance between coagulation and turbulent mixing produces a size distribution at each level which can be considered a mixture of size distributions of differing mean masses and variances. Fig. 4 illustrates this behavior. Again the Cunningham correction to the terminal velocity

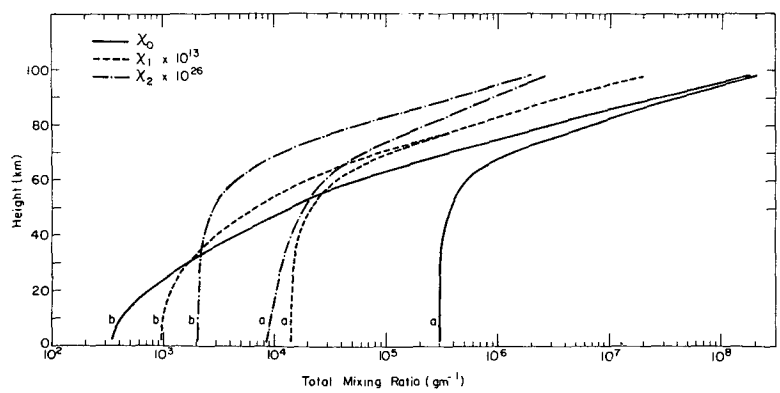

FIG. 4. Comparison of solutions with (b) and without (a) the effects of coagulation included.

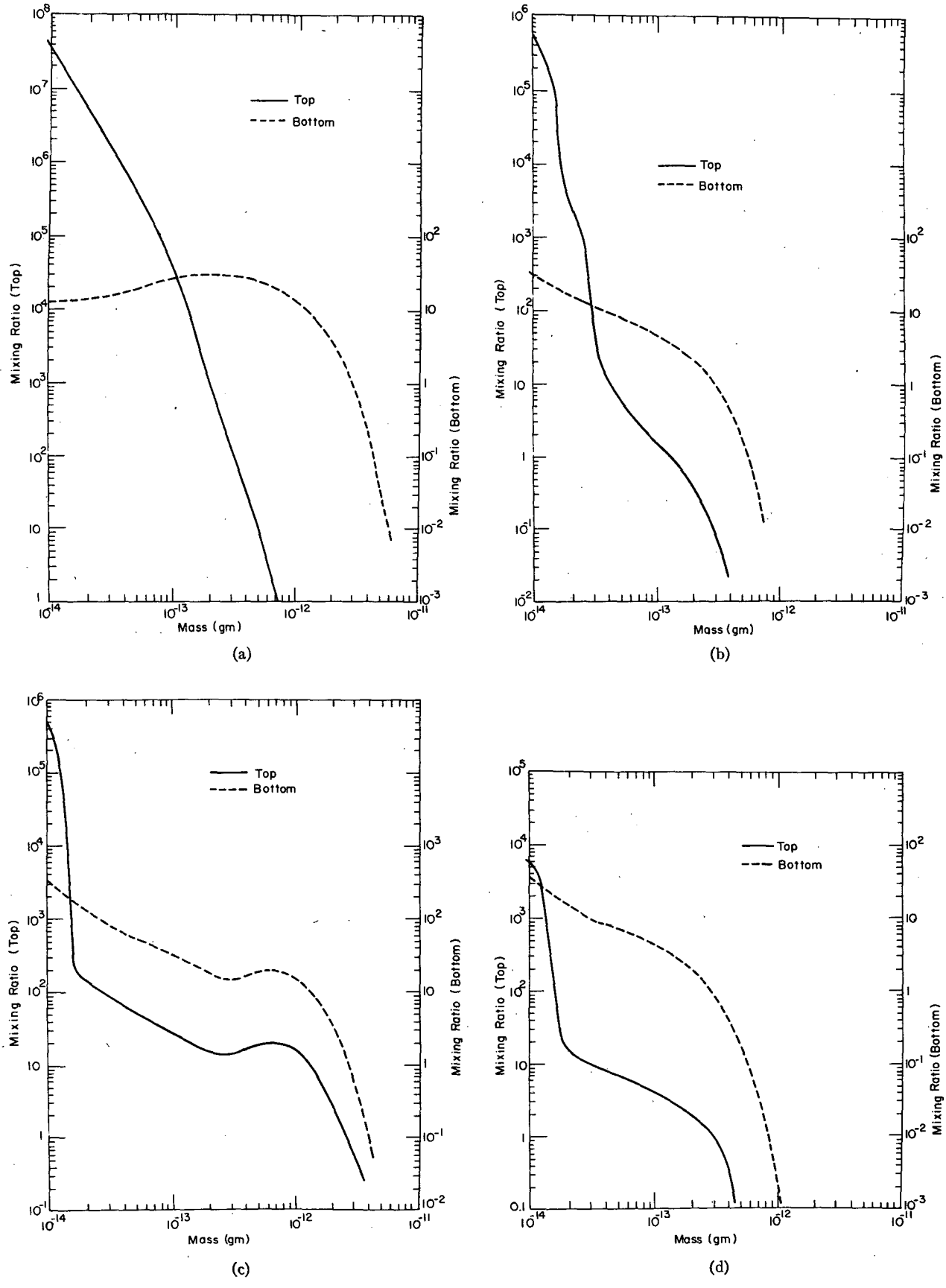

FIG. 5. Particle size distributions at 2 km (dashed lines) and 98 km (solid lines) for exact solution: (a) $E=10^4$ cm^2 s^{-1}, $F_0=1$ cm^{-2} s^{-1}; (b) $E=10^4$ cm^2 s^{-1}, $F_0=10^{-2}$ cm^{-2} s^{-1}; (c) $E=10^6$ cm^2 s^{-1}, $F_0=1$ cm^{-2} s^{-1}; (d) $E=10^6$ cm^2 s^{-1}, $F_0=10^{-2}$ cm^{-2} s^{-1}.

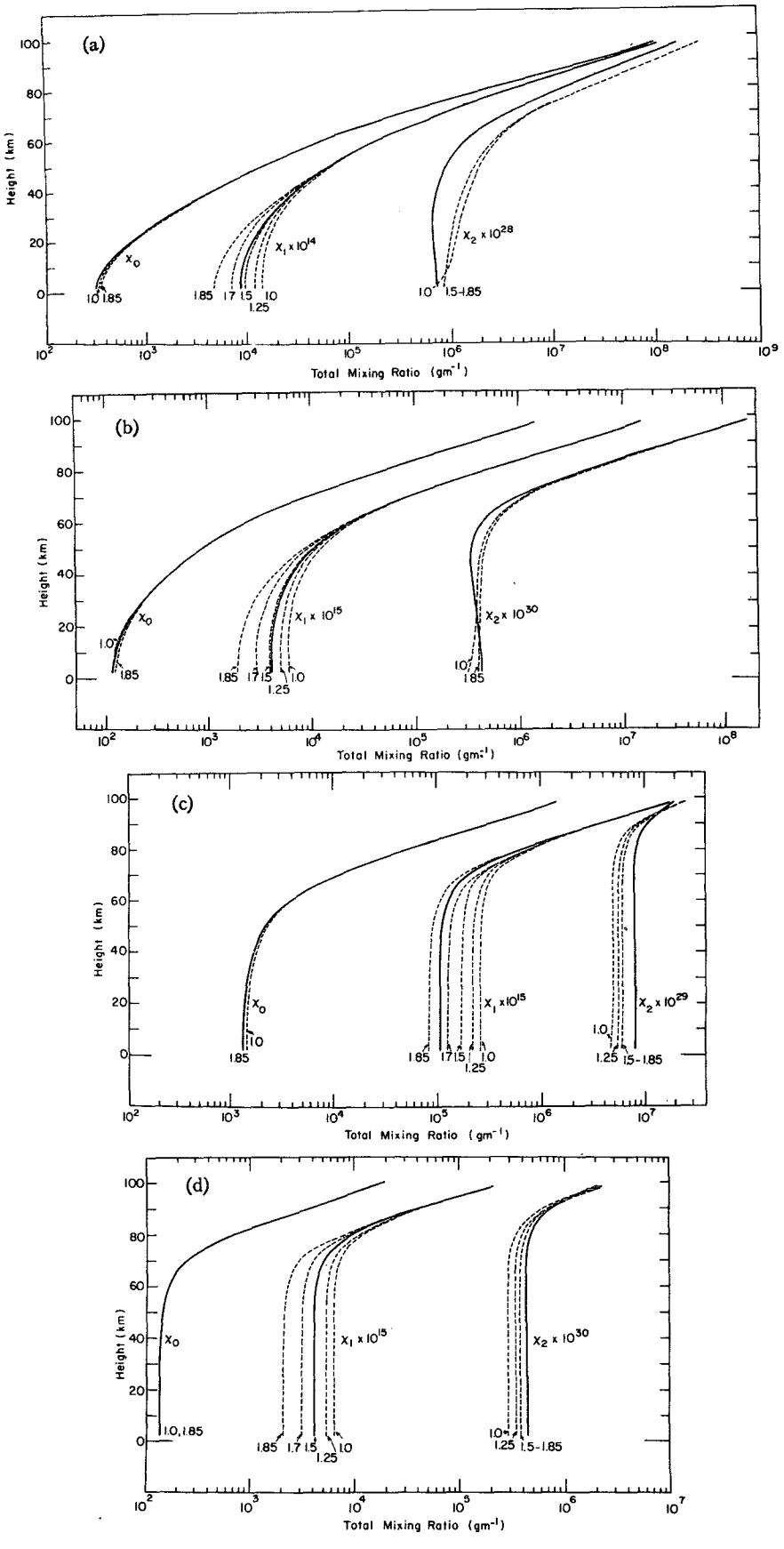

FIG. 6. Comparison of exact and approximate solutions for χ_0, χ_1 and χ_2 for varying values of γ with $f_1 = 1$: values of E and F_0 as in Fig. 5.

has been neglected in order to enhance coagulation in the upper atmosphere.

5. Exact calculations

In order to determine the accuracy of the approximate solution outlined in Sections 2 and 3, solutions of (13) are compared to a numerical solution of Eq. (1) using a discrete size distribution similar to that of Berry and Reinhardt (1974). The partial derivatives in Eq. (1) are approximated by simple, first-order differences and the nonlinear terms are linearized by writing the coefficient as a function of a trial solution. The integral is converted to a sum since the spectrum is assumed to be discrete. The solution to the resulting set of equations is found by inverting the matrix of coefficients, which in this case is tridiagonal. The solution is then used to improve the coefficients and a new solution obtained. This procedure is repeated until the solution stops changing.

The Venus atmosphere thermal structure is that of Marov (1972). The input flux of particles at the top (98 km level) is placed in the smallest two size categories in a $\frac{2}{3}$ and $\frac{1}{3}$ proportion between the smallest and second smallest size. This is necessary in discrete size distribution calculations in order to produce a smooth particle size distribution (Hidy, 1965). Thus the initial size distribution is broader than a delta function. The coagulation coefficient is the size dependent form given by Fuchs (1964) without any correction for the density effects discussed in Section 2a.

For the sake of economy, the size distribution is truncated after 20 categories. The effect produced by this truncation is small if the truncation occurs on the rapidly decreasing tail of the distribution, since the number of particles being neglected is very small (Klett, 1975). This effect was checked by performing some calculations using more size categories and is negligibly small.

Fig. 5 shows the resulting size distributions and the solid lines in Fig. 6 show the results of these calculations in terms of χ_0, χ_1 and χ_2 for the following cases: for $E=10^4$ cm^2 s^{-1}, (a) $F_0=1$ cm^{-2} s^{-1} and (b) $F_0=10^{-2}$ cm^{-2} s^{-1} and for $E=10^6$ cm^2 s^{-1}, (c) $F_0=1$ cm^{-2} s^{-1} and (d) $F_0=10^{-2}$ cm^{-2} s^{-1}. All cases have $V'=V_s$. All of these cases exhibit the transition from constant χ_ν to $\chi_\nu \propto \rho^{-1}$ behavior expected for mixing dominated solutions with sedimentation removal at the surface; however, the effect of coagulation in the lower atmosphere is more pronounced in the weak mixing, high flux case, producing a larger mean mass at the surface. Coagulation is less important in the other cases either as a result of a reduction in the concentration (low flux cases) or as a result of increased transport rate (strong mixing case). The Cunningham correction has been neglected here to enhance coagulation in the upper atmosphere.

Comparison of the particle size distribution for the solutions, displayed in Fig. 5, illustrates the effect of strong mixing on the results. [This figure shows the actual number density at the top and bottom of the atmosphere in each size category rather than the distribution function $n(m,t)$.] The strong mixing size distributions are clearly a mixture of the narrow input distribution from high altitudes with the broad coagulation dominated distribution from near the surface. We note in Table 1 that these size distributions have large values of σ^2.

6. Comparison of solutions

Fig. 6 compares the solutions of Eq. (13) with $f_1=1$, with the Stokes lower boundary condition [Eqs. (19) and (20)] and with varying values for γ to the results presented in Section 5. Eq. (13) was solved by approximating the derivatives by simple, first-order differences. The nonlinear terms are linearized by using trial solutions to calculate the coefficients. The resulting tridiagonal matrix of coefficients is then inverted to obtain a solution, the coefficients are improved, and the process is repeated until the answer stops changing.

TABLE 1. A comparison of the total number of particles per gram of atmosphere χ_0 the mean mass $\langle m \rangle$, and the variance σ^2 of the size distributions at different altitudes in the atmosphere of Venus for different values of the top particle flux F_0 and the eddy diffusivity parameter E for the "exact" and approximate solutions.

			Exact			Approximate		
F_0 (cm^{-2} s^{-1})	E (cm^2 s^{-1})	Location (km)	χ_0 (g^{-1})	$\langle m \rangle$ (g)	σ^2	χ_0 (g^{-1})	$\langle m \rangle$ (g)	σ^2
1.0	10^4	90	2.03×10^{7}	1.37×10^{-14}	0.47	2.60×10^{7}	1.42×10^{-14}	0.51
		2	3.17×10^{2}	2.76×10^{-13}	2.00	3.43×10^{2}	2.80×10^{-13}	1.91
10^{-2}	10^4	90	3.64×10^{5}	9.62×10^{-15}	0.04	3.92×10^{5}	9.63×10^{-15}	0.0
		2	1.16×10^{2}	3.50×10^{-14}	2.12	1.17×10^{2}	3.36×10^{-14}	1.97
1.0	10^6	90	3.80×10^{5}	9.77×10^{-15}	2.06	4.06×10^{5}	9.98×10^{-15}	1.44
		2	1.34×10^{3}	7.81×10^{-14}	8.67	1.48×10^{3}	1.16×10^{-13}	2.02
10^{-2}	10^6	90	3.96×10^{3}	1.02×10^{-14}	0.89	4.19×10^{3}	1.02×10^{-14}	0.72
		2	1.36×10^{5}	3.04×10^{-14}	2.48	1.41×10^{2}	3.00×10^{-14}	2.00
10^2	10^4	90	1.70×10^{6}	1.31×10^{-14}	0.24	4.38×10^{6}	1.37×10^{-14}	0.34
		2	2.31×10^{2}	2.25×10^{-13}	1.65	3.12×10^{2}	2.96×10^{-13}	1.88

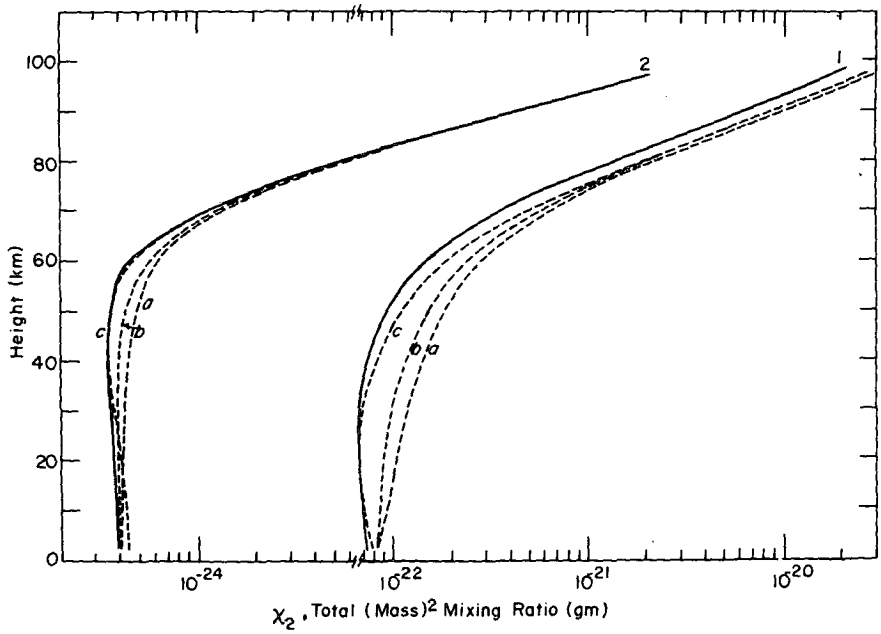

FIG. 7. Variation of χ_2 in approximate solution with differing values of f_1. For curve 1 the assumed flux is 1 cm^{-2} s^{-1} and for curve 2, 10^{-2} cm^{-2} s^{-1}.

It can be seen in Fig. 6 that the best *a priori* guess for γ of 1.5 (halfway between the limiting values) gives good agreement at the surface for all cases. The worst case is for the very broad, bimodal distribution produced by a combination of rapid mixing ($E=10^6$ cm^2 s^{-1}) and rapid coagulation ($F_0=1$ cm^{-2} s^{-1}). Since γ is so insensitive to the actual width of the distribution, $\gamma=1.5$ should always give results at the surface within 50%.

The agreement between values of χ_2 from the "exact" calculations and from these approximate calculations at higher altitudes can be improved by increasing the value of f_1. This behavior is shown in Fig. 7. The importance of the assumed values of f_1 is great only when the mixing is weak, as expected, and a value of $f_1=4$ gives reasonably good results for all the cases considered here. Comparing the results in Figs. 6a, 6b and 7 and in Table 1, we conclude that a factor of 2 uncertainty in f_1 results in less than a factor of 2 uncertainty in χ_2 and that the effect on χ_0 and χ_1 is very much smaller.

The most important fact demonstrated by the comparisons in Fig. 6 is that, despite some disagreement in magnitude, these approximate solutions exhibit the proper qualitative behavior discussed in Section 4. Table 1 compares the values of χ_0 (the total number of particles per gram of atmosphere), $\langle m \rangle$ (the mean mass), and σ^2 (the variance of the size distribution) for the "exact" and approximate calculations. We see that the values of χ_0 and $\langle m \rangle$ are in excellent agreement for all cases. Only σ^2 for cases producing broad, bimodal size distributions is in substantial disagreement. This is to be expected since the first three moments cannot adequately describe a bimodal or more complex distribution.

All of the cases shown here represent cases for which mixing is completely dominant or at least as important as sedimentation in the lower atmosphere. For very weak mixing cases, sedimentation dominates the particle transport even in the lower atmosphere and the solution becomes first order and very sensitive to the choice of f_1. Our approximation and method of solution are not valid for this case. However, for Venus conditions, sedimentation probably does not dominate the transport of particles smaller than about 10 μm in the lower atmosphere and our method can be applied. The last entry in Table 1 shows a case where sedimentation dominates the transport in the upper atmosphere while (weak) mixing dominates in the lower atmosphere. The major cause of difference here is a slight overestimation of the coagulation rate of the smaller particles in the distribution at higher altitudes in the exact calculation.

7. Conclusions

From the results presented in Sections 5 and 6, we conclude that the approximate form (13) of Eq. (1) gives reasonably good values of the first three moments of the aerosol size distribution under Venus conditions. The parameterization of the size dependence of the sedimentation velocity [Eq. (9)] gives results within 50% of the "exact" values for Venus conditions. As Table 1 illustrates, this method is especially accurate for those cases resulting in unimodal size distributions, but still gives good values of the

first two moments even for cases resulting in bimodal size distributions. Some improvement in the values of the third moment might be obtained for more complicated size distributions by extending the system of equations to higher moments. However, since only the first three moments of the Venus cloud size distribution are known from observation, higher accuracy is not warranted.

Solutions for the Stokes bottom boundary condition have been emphasized in this presentation because they represent the least accurate solutions as a result of the approximate boundary condition introduced in Section 3. When V' is independent of particle size, as for turbulent impact deposition or where the magnitude of the solution is specified at the bottom boundary as for a condensate cloud, the technique is more accurate.

The great advantage of this method is its computational economy. While more accurate numerical schemes using explicit size categories require solving a large number (>20) of coupled, nonlinear equations, this method requires solving only a few such equations. In this case, three equations were solved, resulting in a reduction in running time from several minutes to several seconds on an IBM 370/168.

Comparing the first and last entries in Table 1, we see that the number mixing ratio of meteoritic dust in the lower atmosphere of Venus is limited by coagulation. The results in Table 1 can be taken as upper limits on the meteoritic dust density in the lower atmosphere.

Acknowledgments. We thank Michael Belton for his many helpful comments. This work has been supported in part by the Atmospheric Sciences Section of the National Science Foundation under Grant GA-37012.

REFERENCES

Berry, E. X, and R. L. Reinhardt, 1974: An analysis of cloud drop growth by collection: Part I. Double distribution. *J. Atmos. Sci.*, **31**, 1814–1824.

Davies, C. N., 1966: Deposition from moving aerosols. *Aerosol Science*, C. N. Davies, Ed., Academic Press, 393–446.

Dohnanyi, J. S., 1972: Interplanetary objects in review: Statistics of their masses and dynamics. *Icarus*, **17**, 1–48.

Drake, R. L., and T. J. Wright, 1972: The scalar transport equation of coalescence theory: New families of exact solutions. *J. Atmos. Sci.*, **29**, 548–556.

Friedlander, S. K., 1960a: On the particle-size spectrum of atmospheric aerosols. *J. Meteor.*, **17**, 373–374.

——, 1960b: Similarity considerations for the particle-size spectrum of a coagulating, sedimenting aerosol. *J. Meteor.*, **17**, 479–483.

——, 1961: Theoretical considerations for the particle size spectrum of the stratospheric aerosol. *J. Meteor.*, **18**, 753–759.

——, and C. S. Wang, 1966: The self-preserving particle size distribution for coagulation by Brownian motion. *J. Colloid Interface Sci.*, **22**, 126–132.

Fuchs, N. A., 1964: *The Mechanics of Aerosols*. C. N. Davies, Ed., Pergamon Press, 408 pp.

Gillette, D. A., and P. A. Goodwin, 1974: Microscale transport of sand-sized soil aggregates eroded by wind. *J. Geophys. Res.*, **79**, 4080–4084.

——, I. H. Blifford and C. R. Fenster, 1972: Measurements of aerosol size distributions and vertical fluxes of aerosols on land subject to wind erosion, *J. Appl. Meteor.*, **11**, 977–987.

——, ——, and D. W. Fryear, 1974: The influence of wind velocity on the size distribution of aerosols generated by the wind erosion of soils. *J. Geophys. Res.*, **79**, 4068–4075.

Haltiner, G. J., and F. L. Martin, 1957: *Dynamical and Physical Meteorology*. McGraw-Hill, 470 pp.

Hansen, J. E., and J. W. Hovenier, 1974: Interpretation of the polarization of Venus. *J. Atmos. Sci.*, **31**, 1137–1160.

Hidy, G. M., 1965: On the theory of the coagulation of noninteracting particles in Brownian motion. *J. Colloid Interface Sci.*, **20**, 123–144.

——, and J. R. Brock, 1965: Some remarks about the coagulation of aerosol particles by Brownian motion. *J. Colloid Interface Sci.*, **20**, 477–491.

Junge, C. E., 1963: *Air Chemistry and Radioactivity*. Academic Press, 382 pp.

Klett, J. D., 1975: A class of solutions to the steady-state, source-enhanced, kinetic coagulation equation. *J. Atmos. Sci.*, **32**, 380–389.

——, and M. H. Davis, 1973: Theoretical collision efficiencies of cloud droplets at small Reynolds numbers. *J. Atmos. Sci.*, **30**, 107–117.

Liu, B. Y. H., and K. T. Whitby, 1968: Dynamic equilibrium in self-preserving aerosols. *J. Colloid Interface Sci.*, **26**, 161–165.

Marov, M. Ya., 1972: Venus: A perspective at the beginning of planetary exploration. *Icarus*, **16**, 415–461.

——, V. S. Avduevsky, N. F. Borodin, A. P. Ekonomov, V. V. Kerzhanovich, V. P. Lysov, B. Ye. Moshkin, M. K. Rozhdestvensky and O. L. Ryabov, 1973: Preliminary results on the Venus atmosphere from the Venera 8 descent module. *Icarus*, **20**, 407–421.

Mason, B. J., 1971: *The Physics of Clouds*. Clarendon Press, 671 pp.

Mockros, L. F., J. E. Quon and A. T. Hjelmfelt, 1967: Coagulation of a continuously reinforced aerosol. *J. Colloid Interface Sci.*, **23**, 90–98.

Öpik, E. J. 1956: Interplanetary dust and terrestrial accretion of meteoritic matter. *Irish Astron. J.*, 4, 84–135.

Rhee, J. W., 1968: Density of zodiacal dust in interplanetary space. *Origin and Distribution of the Elements*, L. H. Ahrens, Ed., Pergamon Press, 543–546.

Rossow, W. B., 1977: The clouds of Venus: II. An investigation of the influence of coagulation on the observed droplet size distribution. *J. Atmos. Sci.*, **34**, 417–431.

Schneider, E., D. Storzer, J. B. Hartung, H. Fechtig and W. Gentner, 1973: Microcraters on Apollo 15 and 16 samples and corresponding cosmic dust fluxes. *Proc. 4th Lunar Sci. Conf.* (*Geochim. Cosmochim. Acta*), Suppl. 4, Vol. 3, 3277–3290.

Scott, W. T., 1968: Analytic studies of cloud droplet coalescence I. *J. Atmos. Sci.*, **25**, 54–65.

Warshaw, M., 1967: Cloud droplet coalescence: Statistical foundations and a one-dimensional sedimentation model. *J. Atmos. Sci.*, **24**, 278–285.

Young, A. T., 1975: The clouds of Venus. *J. Atmos. Sci.*, **32**, 1125–1132.